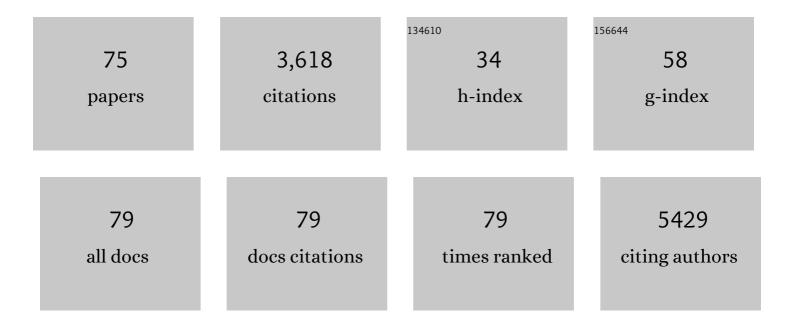
Xuefeng Guo

List of Publications by Year in descending order

Source: https://exaly.com/author-pdf/5025414/publications.pdf Version: 2024-02-01



#	Article	IF	CITATIONS
1	Ultrahigh rate capability of 1D/2D polyaniline/titanium carbide (MXene) nanohybrid for advanced asymmetric supercapacitors. Nano Research, 2022, 15, 285-295.	5.8	50
2	N,O-C Nanocage-mediated high-efficient hydrogen evolution reaction on IrNi@N,O-C electrocatalyst. Applied Catalysis B: Environmental, 2022, 304, 120996.	10.8	34
3	Surface Stability and Morphology of Calcium Phosphate Tuned by pH Values and Lactic Acid Additives: Theoretical and Experimental Study. ACS Applied Materials & Interfaces, 2022, 14, 4836-4851.	4.0	16
4	Overturned Loading of Inert CeO ₂ to Active Co ₃ O ₄ for Unusually Improved Catalytic Activity in Fenton‣ike Reactions. Angewandte Chemie - International Edition, 2022, 61, .	7.2	70
5	Overturned Loading of Inert CeO ₂ to Active Co ₃ O ₄ for Unusually Improved Catalytic Activity in Fentonâ€Like Reactions. Angewandte Chemie, 2022, 134, .	1.6	7
6	Ternary heterostructural CoO/CN/Ni catalyst for promoted CO2 electroreduction to methanol. Journal of Catalysis, 2021, 393, 83-91.	3.1	20
7	High-temperature treatment to engineer the single-atom Pt coordination environment towards highly efficient hydrogen evolution. Journal of Energy Chemistry, 2021, 59, 212-219.	7.1	26
8	Origin of the Activity of Co–N–C Catalysts for Chemoselective Hydrogenation of Nitroarenes. ACS Catalysis, 2021, 11, 3026-3039.	5.5	105
9	Enhanced catalytic activity and stability of bismuth nanosheets decorated by 3-aminopropyltriethoxysilane for efficient electrochemical reduction of CO2. Applied Catalysis B: Environmental, 2021, 298, 120602.	10.8	19
10	Exclusively catalytic oxidation of toluene to benzaldehyde in an O/W emulsion stabilized by hexadecylphosphate acid terminated mixed-oxide nanoparticles. Chinese Journal of Catalysis, 2020, 41, 341-349.	6.9	24
11	Morphologyâ€Reserved Synthesis of Discrete Nanosheets of CuO@SAPOâ€34 and Pore Mouth Catalysis for Oneâ€Pot Oxidation of Cyclohexane. Angewandte Chemie, 2020, 132, 2628-2633.	1.6	12
12	Morphologyâ€Reserved Synthesis of Discrete Nanosheets of CuO@SAPOâ€34 and Pore Mouth Catalysis for Oneâ€Pot Oxidation of Cyclohexane. Angewandte Chemie - International Edition, 2020, 59, 2606-2611.	7.2	36
13	Iron oxide encapsulated in nitrogen-rich carbon enabling high-performance lithium-ion capacitor. Science China Materials, 2020, 63, 2289-2302.	3.5	13
14	CO2 Hydrogenation to Ethanol over Cu@Na-Beta. CheM, 2020, 6, 2673-2689.	5.8	130
15	Crystal-Facet Modulated CrO _{<i>x</i>} /γ-Al ₂ O ₃ : Quasi-Liquid Surface Modification by Bonded Polydimethylsiloxane for Catalytic Oxidation of Propene. Langmuir, 2020, 36, 10404-10411.	1.6	2
16	Surrounded catalysts prepared by ion-exchange inverse loading. Science Advances, 2020, 6, eaay7031.	4.7	17
17	Frontispiece: Morphologyâ€Reserved Synthesis of Discrete Nanosheets of CuO@SAPOâ€34 and Pore Mouth Catalysis for Oneâ€Pot Oxidation of Cyclohexane. Angewandte Chemie - International Edition, 2020, 59, .	7.2	0
18	Full-faradaic-active nitrogen species doping enables high-energy-density carbon-based supercapacitor. Journal of Energy Chemistry, 2020, 48, 277-284.	7.1	140

#	Article	IF	CITATIONS
19	Iron Nanoparticles Encapsulated in S,N-Codoped Carbon: Sulfur Doping Enriches Surface Electron Density and Enhances Electrocatalytic Activity toward Oxygen Reduction. ACS Applied Materials & Interfaces, 2020, 12, 12686-12695.	4.0	39
20	Frontispiz: Morphologyâ€Reserved Synthesis of Discrete Nanosheets of CuO@SAPOâ€34 and Pore Mouth Catalysis for Oneâ€Pot Oxidation of Cyclohexane. Angewandte Chemie, 2020, 132, .	1.6	0
21	Boosting H ₂ Generation Coupled with Selective Oxidation of Methanol into Valueâ€Added Chemical over Cobalt Hydroxide@Hydroxysulfide Nanosheets Electrocatalysts. Advanced Functional Materials, 2020, 30, 1909610.	7.8	190
22	Reactive Template-Derived CoFe/N-Doped Carbon Nanosheets as Highly Efficient Electrocatalysts toward Oxygen Reduction, Oxygen Evolution, and Hydrogen Evolution. ACS Sustainable Chemistry and Engineering, 2019, 7, 15278-15288.	3.2	81
23	The promoted catalytic hydrogenation performance of bimetallic Ni–Co–B noncrystalline alloy nanotubes. RSC Advances, 2019, 9, 26456-26463.	1.7	3
24	Ternary Heterostructural Pt/CNx/Ni as a Supercatalyst for Oxygen Reduction. IScience, 2019, 11, 388-397.	1.9	36
25	Effect of Residual Chlorine on the Catalytic Performance of Co ₃ O ₄ for CO Oxidation. ACS Catalysis, 2019, 9, 11676-11684.	5.5	45
26	Microwave-assisted conversion of biomass wastes to pseudocapacitive mesoporous carbon for high-performance supercapacitor. Journal of Energy Chemistry, 2019, 39, 1-7.	7.1	156
27	A high-performance asymmetric supercapacitor based on vanadyl phosphate/carbon nanocomposites and polypyrrole-derived carbon nanowires. Nanoscale, 2018, 10, 3709-3719.	2.8	36
28	<i>In situ</i> formation/carbonization of quinone-amine polymers towards hierarchical porous carbon foam with high faradaic activity for energy storage. Journal of Materials Chemistry A, 2018, 6, 2353-2359.	5.2	66
29	Pt nanocrystallines/TiO2 with thickness-controlled carbon layers: Preparation and activities in CO oxidation. Chinese Chemical Letters, 2018, 29, 787-790.	4.8	15
30	Facile growth of homogeneous Ni(OH)2 coating on carbon nanosheets for high-performance asymmetric supercapacitor applications. Nano Research, 2018, 11, 216-224.	5.8	189
31	The effect of electrostatic field on the catalytic properties of platinum clusters confined in zeolite for hydrogenation. Catalysis Science and Technology, 2018, 8, 6384-6395.	2.1	18
32	Intercalation of alkylamines in layered MoO ₃ and <i>in situ</i> carbonization for a high-performance asymmetric supercapacitor. Sustainable Energy and Fuels, 2018, 2, 2788-2798.	2.5	21
33	Trimetallic (Co/Ni/Cu) Hydroxyphosphate Nanosheet Array as Efficient and Durable Electrocatalyst for Oxygen Evolution Reaction. ACS Sustainable Chemistry and Engineering, 2018, 6, 16859-16866.	3.2	22
34	Reduction-oxidation pretreatment enhanced catalytic performance of Co3O4/Al2O3 over CO oxidation. Applied Surface Science, 2018, 453, 330-335.	3.1	24
35	Crown ether induced assembly to \hat{I}^3 -Al2O3 nanosheets with rich pentacoordinate Al3+ sites and high ethanol dehydration activity. Applied Surface Science, 2018, 457, 626-632.	3.1	22
36	Surface Sulfurization of NiCo-Layered Double Hydroxide Nanosheets Enable Superior and Durable Oxygen Evolution Electrocatalysis. ACS Applied Energy Materials, 2018, 1, 4040-4049.	2.5	71

#	Article	IF	CITATIONS
37	Crystal-Facet Effect of γ-Al ₂ O ₃ on Supporting CrO _{<i>x</i>} for Catalytic Semihydrogenation of Acetylene. ACS Catalysis, 2018, 8, 6419-6425.	5.5	38
38	Fabrication of TiO ₂ @carbon core–shell nanosheets for advanced lithium-ion batteries with excellent cyclability. Journal of Materials Chemistry A, 2017, 5, 6047-6051.	5.2	30
39	Fabrication of highly dispersed/active ultrafine Pd nanoparticle supported catalysts: a facile solvent-free in situ dispersion/reduction method. Green Chemistry, 2017, 19, 2646-2652.	4.6	24
40	Nanotubular Gamma Alumina with High-Energy External Surfaces: Synthesis and High Performance for Catalysis. ACS Catalysis, 2017, 7, 4083-4092.	5.5	41
41	Two dimensional oxygen-vacancy-rich Co ₃ O ₄ nanosheets with excellent supercapacitor performances. Chemical Communications, 2017, 53, 12410-12413.	2.2	185
42	Distinguishing faceted oxide nanocrystals with 17O solid-state NMR spectroscopy. Nature Communications, 2017, 8, 581.	5.8	48
43	Porous Carbon Nanosheets with Abundant Oxygen Functionalities Derived from Phoenix Seeds for Highâ€Performance Supercapacitor. ChemistrySelect, 2017, 2, 10704-10708.	0.7	14
44	In-Situ-Grown Mg(OH) ₂ -Derived Hybrid α-Ni(OH) ₂ for Highly Stable Supercapacitor. ACS Energy Letters, 2016, 1, 814-819.	8.8	176
45	Ultrathin anatase nanosheets with high energy facets exposed and related photocatalytic performances. RSC Advances, 2016, 6, 62675-62679.	1.7	2
46	Solvent-free synthesis of crystalline mesoporous γ-Fe ₂ O ₃ as an anode material in lithium-ion batteries. RSC Advances, 2016, 6, 57009-57012.	1.7	10
47	S-doped mesoporous nanocomposite of HTiNbO ₅ nanosheets and TiO ₂ nanoparticles with enhanced visible light photocatalytic activity. Physical Chemistry Chemical Physics, 2016, 18, 801-810.	1.3	38
48	Thickness-dependent SERS activities of gold nanosheets controllably synthesized via photochemical reduction in lamellar liquid crystals. Chemical Communications, 2015, 51, 5116-5119.	2.2	28
49	Dehydration and Dehydroxylation of Layered Double Hydroxides: New Insights from Solid-State NMR and FT-IR Studies of Deuterated Samples. Journal of Physical Chemistry C, 2015, 119, 12325-12334.	1.5	36
50	Identification of different oxygen species in oxide nanostructures with ¹⁷ O solid-state NMR spectroscopy. Science Advances, 2015, 1, e1400133.	4.7	72
51	Tri-component noncrystalline Ni–Cu–B nanotubes with enhanced stability and catalytic performance for hydrogenation of p-chlorinitrobenzene. Catalysis Communications, 2015, 64, 66-69.	1.6	10
52	Organic-free synthesis of ultrathin gold nanowires as effective SERS substrates. Chemical Communications, 2015, 51, 11841-11843.	2.2	14
53	Platinum Nanoparticles Encapsulated in MFI Zeolite Crystals by a Two-Step Dry Gel Conversion Method as a Highly Selective Hydrogenation Catalyst. ACS Catalysis, 2015, 5, 6893-6901.	5.5	136
54	A sintering-resistant Pd/SiO ₂ catalyst by reverse-loading nano iron oxide for aerobic oxidation of benzyl alcohol. RSC Advances, 2015, 5, 4766-4769.	1.7	16

#	Article	IF	CITATIONS
55	Catalytic Self-Limited Assembly at Hard Templates: A Mesoscale Approach to Graphene Nanoshells for Lithium–Sulfur Batteries. ACS Nano, 2014, 8, 11280-11289.	7.3	166
56	Investigating Local Structure in Layered Double Hydroxides with ¹⁷ 0 NMR Spectroscopy. Advanced Functional Materials, 2014, 24, 1696-1702.	7.8	32
57	Supramolecular Materials: Investigating Local Structure in Layered Double Hydroxides with170 NMR Spectroscopy (Adv. Funct. Mater. 12/2014). Advanced Functional Materials, 2014, 24, 1695-1695.	7.8	0
58	Ordered nitrogen doped mesoporous carbon assembled under aqueous acidic conditions and its electrochemical capacitive properties. Microporous and Mesoporous Materials, 2014, 197, 237-243.	2.2	34
59	Partially nitrided molybdenum trioxide with promoted performance as an anode material for lithium-ion batteries. Journal of Materials Chemistry A, 2014, 2, 699-704.	5.2	104
60	Organoamine-assisted biomimetic synthesis of faceted hexagonal hydroxyapatite nanotubes with prominent stimulation activity for osteoblast proliferation. Journal of Materials Chemistry B, 2014, 2, 1760-1763.	2.9	41
61	Expeditious fabrication of flower-like hierarchical mesoporous carbon superstructures as supercapacitor electrode materials. Journal of Materials Chemistry A, 2014, 2, 16884-16891.	5.2	66
62	Probing Local Structure of Layered Double Hydroxides with ¹ H Solid-State NMR Spectroscopy on Deuterated Samples. Journal of Physical Chemistry Letters, 2014, 5, 363-369.	2.1	16
63	In situ hydrothermal deposition as an efficient catalyst supporting method towards low-temperature graphitization of amorphous carbon. Carbon, 2014, 77, 215-225.	5.4	78
64	High performance catalytic distillation using CNTs-based holistic catalyst for production of high quality biodiesel. Scientific Reports, 2014, 4, 4021.	1.6	20
65	High performance mesoporous zirconium phosphate for dehydration of xylose to furfural in aqueous-phase. RSC Advances, 2013, 3, 23228.	1.7	42
66	Synergism between the Lewis and Brönsted acid sites on HZSM-5 zeolites in the conversion of methylcyclohexane. Chinese Journal of Catalysis, 2013, 34, 2153-2159.	6.9	22
67	Sandwich-like LiFePO4/graphene hybrid nanosheets: in situ catalytic graphitization and their high-rate performance for lithium ion batteries. Journal of Materials Chemistry A, 2013, 1, 11534.	5.2	81
68	Facile strategy for synthesis of mesoporous crystalline Î ³ -alumina by partially hydrolyzing aluminum nitrate solution. Journal of Materials Chemistry, 2012, 22, 23806.	6.7	45
69	Noncrystalline NiPB nanotubes for hydrogenation of p-chloronitrobenzene. Chemical Communications, 2010, 46, 2268.	2.2	31
70	Preparation and catalytic property of a non-crystalline alloy of iron–boron with one-dimensional nanostructures. Nanotechnology, 2007, 18, 195601.	1.3	10
71	Controllable synthesis of CuS nanotubes and nanobelts using lyotropic liquid crystal templates. Journal of Materials Science, 2007, 42, 1042-1045.	1.7	21
72	Noncrystalline Metal–Boron Nanotubes: Synthesis, Characterization, and Catalytic-Hydrogenation Properties. Angewandte Chemie - International Edition, 2006, 45, 7211-7214.	7.2	51

#	Article	IF	CITATIONS
73	Novel Coassembly Route to Cuâ^'SiO2MCM-41-like Mesoporous Materials. Langmuir, 2004, 20, 2879-2882.	1.6	23
74	Synthesis of a novel mesoporous iron phosphate. Chemical Communications, 2001, , 709-710.	2.2	48
75	Sandwich-Like Holey Graphene/PANI/Graphene Nanohybrid for Ultrahigh-Rate Supercapacitor. ACS Applied Energy Materials, 0, , .	2.5	14